Next-to-next-to-leading order soft-gluon corrections in top quark hadroproduction

Nikolaos Kidonakis
Cavendish Laboratory, University of Cambridge, Madingley Road, Cambridge CB3 0HE, United Kingdom

Ramona Vogt
Nuclear Science Division, Lawrence Berkeley National Laboratory, Berkeley, California 94720, USA
and Physics Department, University of California at Davis, Davis, California 95616, USA
(Received 22 August 2003; published 30 December 2003)

We calculate next-to-next-to-leading order soft-gluon corrections to top quark total and differential cross sections in hadron colliders. We increase the accuracy of our previous estimates by including additional subleading terms, including next-to-next-to-next-to-leading-logarithmic and some virtual terms. We show that the kinematics dependence of the cross section vanishes near threshold and is reduced away from it. The factorization and renormalization scale dependence of the cross section is also greatly reduced. We present results for the top quark total cross sections and transverse momentum distributions at the Fermilab Tevatron and the CERN LHC.

DOI: 10.1103/PhysRevD.68.114014 PACS number(s): 12.38.Bx

I. INTRODUCTION

The discovery of the top quark in $p\bar{p}$ collisions at run I of the Fermilab Tevatron in 1995 [1] and its observation currently at run II, with expected increases in the accuracy of the top mass and cross section measurements, have made theoretical calculations of top production cross sections and differential distributions an interesting and topical subject. The latest calculation for top hadroproduction includes next-to-next-to-leading-order (NNLO) soft-gluon corrections to the double differential cross section [2,3] from threshold resummation techniques [4–10]. Near threshold there is limited phase space for the emission of real gluons so that soft-gluon corrections dominate the cross section.

These soft corrections take the form of logarithms, $[\ln^l(x_{\rm th})/x_{\rm th}]_+$, with $l \leqslant 2n-1$ for the order α_s^n corrections, where $x_{\rm th}$ is a kinematical variable that measures distance from threshold and goes to zero at threshold. NNLO calculations for top quark production have so far been done through next-to-next-to-leading-logarithmic (NNLL) accuracy, i.e., for the scale-independent terms, including leading logarithms (LL) with $l=3$, next-to-leading logarithms (NLL) with $l=2$, and NNLL with $l=1$ [2,3]. This NNLO-NNLL calculation has had great success in significantly reducing the factorization or renormalization scale dependence of the cross section. Indeed the scale dependence of top production is almost negligible. However, the dependence of the corrections on the kinematics choice is substantial. In Ref. [3], the top cross section was studied in both single-particle-inclusive (1PI) and pair-invariant-mass (PIM) kinematics. Important differences between the two kinematics choices were found in both the parton-level and hadron-level cross sections, even near threshold. Similar kinematics effects were found for bottom and charm hadroproduction [3,11]. Thus subleading, beyond NNLL, contributions can still have an impact on the cross section. If all the NNLO soft corrections are included, there should be no difference between the two kinematics near threshold. If all NNLO corrections, both soft and hard, were known, there should be no difference between the two kinematics, even far from threshold. Away from threshold, where the approximations of Ref. [3] are not expected to apply since real emission of hard gluons comes into play, the discrepancy between the 1PI and PIM results is not surprising. However, the NNLO-NNLL calculation exhibits some notable discrepancies between the two kinematics even at the lowest η, where $\eta = s/(4m^2)-1 \to 0$ at threshold. Thus, additional subleading terms are clearly needed to bring the calculation under further theoretical control.

In this paper, we include additional subleading NNLO soft corrections, including next-to-next-to-next-to-leading logarithms (NNNLL), as well as some virtual $\delta(x_{\rm th})$ corrections. We apply the method and results of Ref. [12], based on earlier resummation studies [4–6], where master formulas are given for the NNLO soft and virtual corrections for processes in hadron-hadron and lepton-hadron collisions. As we will see, the subleading corrections do indeed bring the 1PI and PIM results into agreement near threshold for both the $q\bar{q} \to t\bar{t}$ and the $gg \to t\bar{t}$ channels, while the discrepancies away from threshold are also diminished, especially in the gg channel. Thus the threshold region is brought under theoretical control.

Since the resummation formalism has been reviewed extensively in Refs. [2–5,12], we only provide a rough outline here. Threshold resummation is a method of formally calculating contributions from soft-gluon emission to all orders in perturbation theory. The resummation is normally carried out in moment space where N is the variable conjugate to $x_{\rm th}$ and the leading threshold logarithms are of the form $\ln^{2n}N$ for the order α_s^n corrections. The resummed cross section, in moment space, can then be expanded to NNLO (and even higher orders [2]) and the finite-order result finally inverted back to momentum space. The previous calculations of Refs. [2,3] and the universal results of Ref. [12] employ this approach.

In the following section, we briefly discuss the difference between 1PI and PIM kinematics choices and introduce the scaling functions comprising the partonic cross sections employed later. Then in Sec. III, we give the analytical form of the NNLO soft and (some) virtual corrections in the $q\bar{q}\to t\bar{t}$ channel in both 1PI and PIM kinematics. In Sec. IV we give the corresponding results for the $gg\to t\bar{t}$ channel. Note that while we refer only to $t\bar{t}$ here, the results in Secs. III and IV are equally valid for all heavy quarks. Section V discusses the partonic cross sections in both channels. In Sec. VI we present the hadronic cross sections and transverse momentum distributions for top production in Tevatron run I and run II as well as at the LHC. We conclude with a summary in Sec. VII.

II. KINEMATICS AND SCALING FUNCTIONS

We study the partonic process $ij\to t\bar{t}$. Before discussing the corrections, we introduce our kinematics notation. The same notation is used for $ij=q\bar{q}$ and gg. A more detailed discussion of the kinematics can be found in Ref. [3].

In 1PI kinematics, a single top quark is identified, so that

$$i(p_a)+j(p_b)\to t(p_1)+X[\bar{t}](p_2) \tag{2.1}$$

where t is the identified top quark of mass m and $X[\bar{t}]$ is the remaining final state that contains the $\bar{t}$. We define the kinematical invariants $s=(p_a+p_b)^2$, $t_1=(p_b-p_1)^2-m^2$, $u_1=(p_a-p_1)^2-m^2$ and $s_4=s+t_1+u_1$. At threshold, $s_4\to 0$, and the soft corrections appear as $[\ln^l(s_4/m^2)/s_4]_+$.

In PIM kinematics, we have instead

$$i(p_a)+j(p_b)\to t\bar{t}(p)+X(k). \tag{2.2}$$

At partonic threshold, $s=M^2$, M^2 is the pair mass squared, $t_1=-(M^2/2)(1-\beta_M\cos\theta)$, and $u_1=-(M^2/2)(1+\beta_M\cos\theta)$ where $\beta_M=\sqrt{1-4m^2/M^2}$ and θ is the scattering angle in the parton-parton center-of-mass frame. The soft corrections appear as $[\ln^l(1-z)/(1-z)]_+$ with $z=M^2/s\to 1$ at threshold.

At leading order (LO) the partonic threshold condition is exact and there is no difference between the total cross sections in the two kinematic schemes. However, beyond LO additional soft partons are produced and there is a difference when not all terms are known. Any difference in the integrated cross sections due to kinematics choice thus arises from uncalculated subleading terms. The total partonic cross section may be expressed in terms of dimensionless scaling functions $f_{ij}^{(k,r)}$ that depend only on the variable $\eta=s/4m^2-1$ [3],

$$\sigma_{ij}(s,m^2,\mu^2)=\frac{\alpha_s^2(\mu)}{m^2}\sum_{k=0}^{\infty}(4\pi\alpha_s(\mu))^k \times\sum_{r=0}^{k} f_{ij}^{(k,r)}(\eta)\ln^r\left(\frac{\mu^2}{m^2}\right). \tag{2.3}$$

Previously, we constructed LL, NLL, and NNLL approximations to $f_{ij}^{(k,r)}$ in the $q\bar{q}$ and gg channels for $k\le 2$, $r\le k$ [3]. The renormalization and factorization scales, μ_R and μ_F respectively, enter the partonic cross section in powers of $\ln(\mu^2/m^2)$, multiplying the scaling functions. For convenience, we write $\mu\equiv\mu_F=\mu_R$ here but retain the specific dependence in Secs. III and IV. We work in the $\overline{\rm MS}$ scheme throughout.

The scaling functions contain the information on the kinematics dependence of the partonic cross sections. To NNLL, the results presented in the following sections are identical to those of Ref. [3]. Only the notation has been made more compact. Thus the $f_{ij}^{(2,2)}$ scaling function, already at NNLL with the virtual $\delta(x_{\rm th})$ contributions, is thus unchanged from Ref. [3]. In this paper we calculate $f_{ij}^{(2,1)}$ to NNNLL, including the $\delta(x_{\rm th})$ contributions, and, for $f_{ij}^{(2,0)}$, the NNNLL $[1/x_{\rm th}]_+$ and some virtual $\delta(x_{\rm th})$ contributions. These new contributions are identified more explicitly in the following sections.

III. NNLO SOFT CORRECTIONS TO $q\bar{q}\to t\bar{t}$

A. The $q\bar{q}\to t\bar{t}$ channel in 1PI kinematics

We begin our study with the next-to-leading order (NLO) corrections. In the $\overline{\rm MS}$ scheme, the NLO soft and virtual corrections for $q\bar{q}\to t\bar{t}$ in 1PI kinematics can be written as

$$s^2\frac{d^2\hat{\sigma}_{q\bar{q}}^{(1)\,\rm 1PI}}{dt_1\,du_1}=F^{B\,\rm 1PI}_{q\bar{q}}\frac{\alpha_s(\mu_R^2)}{\pi}\left\{c^{\rm 1PI}_{3\,q\bar{q}}\left[\frac{\ln(s_4/m^2)}{s_4}\right]_+ +c^{\rm 1PI}_{2\,q\bar{q}}\left[\frac{1}{s_4}\right]_+ +c^{\rm 1PI}_{1\,q\bar{q}}\delta(s_4)\right\}. \tag{3.1}$$

Here the Born term is

$$F^{B\,\rm 1PI}_{q\bar{q}}=\pi\alpha_s^2(\mu_R^2)K_{q\bar{q}}N_cC_F\left[\frac{t_1^2+u_1^2}{s^2}+\frac{2m^2}{s}\right] \tag{3.2}$$

where $C_F=(N_c^2-1)/(2N_c)$ with $N_c=3$ the number of colors, and $K_{q\bar{q}}=N_c^{-2}$ is a color average factor. Equation (3.1), written in the compact notation of Ref. [12], is identical to Eq. (B2) of Ref. [3].

We also have $c^{\rm 1PI}_{3\,q\bar{q}}=4C_F$ and

$$c^{\rm 1PI}_{2\,q\bar{q}}=2C_F\left[4\ln\left(\frac{u_1}{t_1}\right)-\ln\left(\frac{t_1u_1}{m^4}\right)-L'_\beta-1-\ln\left(\frac{\mu_F^2}{s}\right)\right] +C_A\left[-3\ln\left(\frac{u_1}{t_1}\right)-\ln\left(\frac{m^2s}{t_1u_1}\right)+L'_\beta\right], \tag{3.3}$$

where $C_A = N_c$, $L'_\beta = [(1-2m^2/s)/\beta]\ln[(1-\beta)/(1+\beta)]$ and $\beta = \sqrt{1-4m^2/s}$. For later use, we write

$$c_{2\,q\bar{q}}^{1\mathrm{PI}} \equiv T_{2\,q\bar{q}}^{1\mathrm{PI}} - 2C_F \ln\left(\frac{\mu_F^2}{s}\right), \tag{3.4}$$

so that $T_{2\,q\bar{q}}^{1\mathrm{PI}}$ is the scale-independent part of $c_{2\,q\bar{q}}^{1\mathrm{PI}}$. Finally,

$$c_{1\,q\bar{q}}^{1\mathrm{PI}} = \frac{\sigma_{q\bar{q}\delta}^{(1)S+V\ 1\mathrm{PI}}}{(\alpha_s/\pi) F_{q\bar{q}}^{B\ 1\mathrm{PI}}} \tag{3.5}$$

where $\sigma_{q\bar{q}\delta}^{(1)S+V\ 1\mathrm{PI}}$ denotes the $\delta(s_4)$ terms in Eq. (4.7) of Ref. [13] with the definitions of t_1 and u_1 interchanged with respect to that reference. We also write

$$c_{1\,q\bar{q}}^{1\mathrm{PI}} \equiv T_{1\,q\bar{q}}^{1\mathrm{PI}} + C_F\left[-\frac{3}{2} + \ln\left(\frac{t_1 u_1}{m^4}\right)\right]\ln\left(\frac{\mu_F^2}{s}\right) + \frac{\beta_0}{2}\ln\left(\frac{\mu_R^2}{s}\right), \tag{3.6}$$

where $T_{1\,q\bar{q}}^{1\mathrm{PI}}$ has no scale dependence.

Before presenting the NNLO soft corrections, we define the constants $\zeta_2 = \pi^2/6$, $\zeta_4 = \pi^4/90$, and $\zeta_3 = 1.2020569\ldots$, and the two-loop constant $K = C_A(67/18 - \pi^2/6) - 5n_f/9$, with n_f the number of light quark flavors. Finally, we define

$$\beta(\alpha_s) \equiv \mu\frac{d\ln g}{d\mu} = -\beta_0\frac{\alpha_s}{4\pi} - \beta_1\frac{\alpha_s^2}{(4\pi)^2} + \cdots, \tag{3.7}$$

where $\beta_0 = (11C_A - 2n_f)/3$ and

$$\beta_1 = \frac{34}{3}C_A^2 - 2n_f\left(C_F + \frac{5}{3}C_A\right). \tag{3.8}$$

Following Ref. [12] we write the NNLO soft-plus-virtual corrections, including subleading terms, in 1PI kinematics as

$$\begin{aligned}
s^2\frac{d^2\hat{\sigma}_{q\bar{q}}^{(2)\ 1\mathrm{PI}}}{dt_1\,du_1} = F_{q\bar{q}}^{B\ 1\mathrm{PI}}\frac{\alpha_s^2(\mu_R^2)}{\pi^2}\Bigg\{ & \frac{1}{2}(c_{3\,q\bar{q}}^{1\mathrm{PI}})^2\left[\frac{\ln^3(s_4/m^2)}{s_4}\right]_+ + \left[\frac{3}{2}c_{3\,q\bar{q}}^{1\mathrm{PI}}c_{2\,q\bar{q}}^{1\mathrm{PI}} - \frac{\beta_0}{4}c_{3\,q\bar{q}}^{1\mathrm{PI}}\right]\left[\frac{\ln^2(s_4/m^2)}{s_4}\right]_+ \\
& + \left[c_{3\,q\bar{q}}^{1\mathrm{PI}}c_{1\,q\bar{q}}^{1\mathrm{PI}} + (c_{2\,q\bar{q}}^{1\mathrm{PI}})^2 - \zeta_2(c_{3\,q\bar{q}}^{1\mathrm{PI}})^2 - \frac{\beta_0}{2}T_{2\,q\bar{q}}^{1\mathrm{PI}} + \frac{\beta_0}{4}c_{3\,q\bar{q}}^{1\mathrm{PI}}\ln\left(\frac{\mu_R^2}{s}\right) + 2C_F K + 8\frac{C_F}{C_A}\ln^2\left(\frac{u_1}{t_1}\right)\right]\left[\frac{\ln(s_4/m^2)}{s_4}\right]_+ \\
& + \Bigg[c_{2\,q\bar{q}}^{1\mathrm{PI}}c_{1\,q\bar{q}}^{1\mathrm{PI}} - \zeta_2 c_{2\,q\bar{q}}^{1\mathrm{PI}}c_{3\,q\bar{q}}^{1\mathrm{PI}} + \zeta_3(c_{3\,q\bar{q}}^{1\mathrm{PI}})^2 - \frac{\beta_0}{2}T_{1\,q\bar{q}}^{1\mathrm{PI}} + \frac{\beta_0}{4}c_{2\,q\bar{q}}^{1\mathrm{PI}}\ln\left(\frac{\mu_R^2}{s}\right) + \mathcal{G}_{q\bar{q}}^{(2)} + C_F\frac{\beta_0}{4}\ln^2\left(\frac{\mu_F^2}{s}\right) \\
& - C_F K\ln\left(\frac{\mu_F^2}{s}\right) - C_F K\ln\left(\frac{t_1 u_1}{m^4}\right) + 8\frac{C_F}{C_A}\ln^2\left(\frac{u_1}{t_1}\right)\ln\left(\frac{m^2}{s}\right)\Bigg]\left[\frac{1}{s_4}\right]_+ + R_{q\bar{q}}^{1\mathrm{PI}}\delta(s_4)\Bigg\}.
\end{aligned} \tag{3.9}$$

Here

$$\mathcal{G}_{q\bar{q}}^{(2)} = C_F C_A\left(\frac{7}{2}\zeta_3 + \frac{22}{3}\zeta_2 - \frac{299}{27}\right) + n_f C_F\left(-\frac{4}{3}\zeta_2 + \frac{50}{27}\right) \tag{3.10}$$

denotes a set of two-loop contributions that are universal for processes with $q\bar{q}$ initial states [12]. Process-dependent two-loop corrections [14] are not included in $\mathcal{G}_{q\bar{q}}^{(2)}$ but, as we will see in Sec. V, their contribution is expected to be negligible.

Up to NNLL, the results in Eq. (3.9) are identical to the sum of Eqs. (B3) and (B4) in Ref. [3]. The scale-independent terms multiplying $[1/s_4]_+$ are proportional to the new NNNLL contribution to $f_{ij}^{(2,0)}$ in 1PI kinematics. The relationship is not exact because the prefactors in Eq. (2.3) must be correctly accounted for. Note that in Eq. (2.3), the scale-dependent terms are written as $\ln(\mu^2/m^2)$. This is done simply by making the substitution $\ln(\mu^2/s) = \ln(\mu^2/m^2) + \ln(m^2/s)$ and incorporating the additional $\ln(m^2/s)$ terms into the scale-independent contribution.

The virtual contribution $R_{q\bar{q}}^{1\mathrm{PI}}$ is not fully known. However, we can determine certain terms in $R_{q\bar{q}}^{1\mathrm{PI}}$ exactly. The exact terms involving the factorization and renormalization scales are the NNLL contribution to $f_{q\bar{q}}^{(2,2)}$ and the NNNLL contribution to $f_{q\bar{q}}^{(2,1)}$. The scale-independent contributions to $f_{q\bar{q}}^{(2,0)}$ arise from the inversion from moment to momentum space. These virtual ζ terms are subleading relative to the NNNLL contribution to $f_{q\bar{q}}^{(2,0)}$. (For a detailed discussion of the inversion procedure see Sec. III C and Appendix A of Ref. [2].)

The terms multiplying $\delta(s_4)$ involving the factorization and renormalization scales are given explicitly by

$$F^{B\_1\mathrm{PI}}_{q\bar{q}}\frac{\alpha_s^2(\mu_R^2)}{\pi^2}\left[\ln^2\left(\frac{\mu_F^2}{m^2}\right)\left\{\frac{C_F^2}{2}\left[\ln\left(\frac{t_1u_1}{m^4}\right)-\frac{3}{2}\right]^2-2\zeta_2C_F^2+\frac{\beta_0}{8}C_F\left[\frac{3}{2}-\ln\left(\frac{t_1u_1}{m^4}\right)\right]\right\}\right.$$
$$+\ln\left(\frac{\mu_F^2}{m^2}\right)\ln\left(\frac{\mu_R^2}{m^2}\right)\frac{3\beta_0}{4}C_F\left[\ln\left(\frac{t_1u_1}{m^4}\right)-\frac{3}{2}\right]+\ln^2\left(\frac{\mu_R^2}{m^2}\right)\frac{3\beta_0^2}{16}$$
$$+\ln\left(\frac{\mu_F^2}{m^2}\right)\left\{C_F^2\left[\ln\left(\frac{t_1u_1}{m^4}\right)-\frac{3}{2}\right]^2\ln\left(\frac{m^2}{s}\right)+C_F\left[\ln\left(\frac{t_1u_1}{m^4}\right)-\frac{3}{2}\right]\left[T^{1\mathrm{PI}}_{1\,q\bar{q}}+\frac{\beta_0}{2}\ln\left(\frac{m^2}{s}\right)\right]\right.$$
$$\left.+2C_F\zeta_2\left[T^{1\mathrm{PI}}_{2\,q\bar{q}}-2C_F\ln\left(\frac{m^2}{s}\right)\right]-8C_F^2\zeta_3+C_F\frac{K}{2}\ln\left(\frac{t_1u_1}{m^4}\right)-2\gamma'^{(2)}_{q/q}\right\}$$
$$\left.+\ln\left(\frac{\mu_R^2}{m^2}\right)\left\{\frac{3\beta_0}{4}\left[C_F\left(\ln\left(\frac{t_1u_1}{m^4}\right)-\frac{3}{2}\right)\ln\left(\frac{m^2}{s}\right)+\frac{\beta_0}{2}\ln\left(\frac{m^2}{s}\right)+T^{1\mathrm{PI}}_{1\,q\bar{q}}\right]+\frac{\beta_1}{8}\right\}\right] \tag{3.11}$$

where

$$\gamma'^{(2)}_{q/q}=C_F^2\left(\frac{3}{32}-\frac{3}{4}\zeta_2+\frac{3}{2}\zeta_3\right)+C_FC_A\left(-\frac{3}{4}\zeta_3+\frac{11}{12}\zeta_2+\frac{17}{96}\right)+n_fC_F\left(-\frac{\zeta_2}{6}-\frac{1}{48}\right). \tag{3.12}$$

The contributions multiplying quadratic powers of $\ln(\mu^2/m^2)$ are proportional to $f^{(2,2)}_{q\bar{q}}$ while those linear in $\ln(\mu^2/m^2)$ are proportional to the new NNNLL contributions to $f^{(2,1)}_{q\bar{q}}$ in 1PI kinematics.

The terms multiplying $\delta(s_4)$ resulting from inversion (ζ terms) that do not involve the factorization and renormalization scales are [2,12]

$$F^{B\_1\mathrm{PI}}_{q\bar{q}}\frac{\alpha_s^2(\mu_R^2)}{\pi^2}\left\{-\frac{\zeta_2}{2}\left[T^{1\mathrm{PI}}_{2\,q\bar{q}}-2C_F\ln\left(\frac{m^2}{s}\right)\right]^2+\frac{1}{4}\zeta_2^2(c^{1\mathrm{PI}}_{3\,q\bar{q}})^2+\zeta_3c^{1\mathrm{PI}}_{3\,q\bar{q}}\left[T^{1\mathrm{PI}}_{2\,q\bar{q}}-2C_F\ln\left(\frac{m^2}{s}\right)\right]-\frac{3}{4}\zeta_4(c^{1\mathrm{PI}}_{3\,q\bar{q}})^2-4\zeta_2\frac{C_F}{C_A}\ln^2\left(\frac{u_1}{t_1}\right)\right\}. \tag{3.13}$$

These are the new virtual ζ contributions proportional to $f^{(2,0)}_{q\bar{q}}$ in 1PI kinematics.

B. The $q\bar{q}\to t\bar{t}$ channel in PIM kinematics

Next, we study the soft-gluon corrections in PIM kinematics. The $\overline{\mathrm{MS}}$ NLO soft and virtual corrections to $q\bar{q}\to t\bar{t}$ in PIM kinematics are

$$s\frac{d^2\hat{\sigma}^{(1)\,\mathrm{PIM}}_{q\bar{q}}}{dM^2d\cos\theta}=F^{B\_\mathrm{PIM}}_{q\bar{q}}\frac{\alpha_s(\mu_R^2)}{\pi}\left\{c^{\mathrm{PIM}}_{3\,q\bar{q}}\left[\frac{\ln(1-z)}{1-z}\right]_+ +c^{\mathrm{PIM}}_{2\,q\bar{q}}\left[\frac{1}{1-z}\right]_+ +c^{\mathrm{PIM}}_{1\,q\bar{q}}\delta(1-z)\right\}. \tag{3.14}$$

Here the Born term is

$$F^{B\_\mathrm{PIM}}_{q\bar{q}}=\frac{\beta}{2s}F^{B\_1\mathrm{PI}}_{q\bar{q}}|_{\mathrm{PIM}}=\frac{\beta}{2s}\pi\alpha_s^2K_{q\bar{q}}N_cC_F\left[\frac{1}{2}(1+\beta^2\cos^2\theta)+\frac{2m^2}{s}\right], \tag{3.15}$$

where $|_{\mathrm{PIM}}$ indicates that for t_1, u_1 we use the expressions below Eq. (2.2). Equation (3.14), written in the notation of Ref. [12], is identical to Eq. (B16) of Ref. [3].

Also $c^{\mathrm{PIM}}_{3\,q\bar{q}}=4C_F$,

$$c^{\mathrm{PIM}}_{2\,q\bar{q}}=2C_F\left[4\ln\left(\frac{u_1}{t_1}\right)-L'_\beta-1-\ln\left(\frac{\mu_F^2}{s}\right)\right]+C_A\left[-3\ln\left(\frac{u_1}{t_1}\right)-\ln\left(\frac{m^2s}{t_1u_1}\right)+L'_\beta\right],$$
$$\equiv T^{\mathrm{PIM}}_{2\,q\bar{q}}-2C_F\ln\left(\frac{\mu_F^2}{s}\right), \tag{3.16}$$

and

$$c^{\mathrm{PIM}}_{1\,q\bar{q}}\equiv T^{\mathrm{PIM}}_{1\,q\bar{q}}-\frac{3}{2}C_F\ln\left(\frac{\mu_F^2}{s}\right)+\frac{\beta_0}{2}\ln\left(\frac{\mu_R^2}{s}\right). \tag{3.17}$$

Note that the scale-independent $T^{\mathrm{PIM}}_{1\,q\bar{q}}$ is related to its 1PI counterpart by

$$T_{1\,q\bar{q}}^{\mathrm{PIM}}=2T_{1\,q\bar{q}}^{1\mathrm{PI}}\Big|_{\mathrm{PIM}}+\frac{1}{F_{q\bar{q}}^{B\_\mathrm{PIM}}}s\frac{d^2\sigma'^{(1)\ \mathrm{S+MF}}_{q\bar{q}}}{dM^2 d\cos\theta}-\frac{1}{F_{q\bar{q}}^{B\_\mathrm{PIM}}}\frac{\beta}{s}s^2\frac{d^2\sigma'^{(1)\ \mathrm{S+MF}}_{q\bar{q}}}{dt_1 du_1}\Bigg|_{\mathrm{PIM}}. \tag{3.18}$$

Here $\sigma'^{(1)\ \mathrm{S+MF}}_{q\bar{q}}$ denotes the soft and mass factorization subtraction terms calculated in Ref. [3]. The prime indicates that we drop the overall $\delta(1-z)$ or $\delta(s_4)$ coefficient from the expressions in Eqs. (82), (A8), and (A9) of Ref. [3].

In PIM kinematics, the NNLO soft-plus-virtual corrections, including the new subleading terms, are

$$\begin{aligned}
s\frac{d^2\hat{\sigma}^{(2)\ \mathrm{PIM}}_{q\bar{q}}}{dM^2 d\cos\theta}=F_{q\bar{q}}^{B_\mathrm{PIM}}\frac{\alpha_s^2(\mu_R^2)}{\pi^2}\Bigg\{&\frac{1}{2}(c_{3\,q\bar{q}}^{\mathrm{PIM}})^2\left[\frac{\ln^3(1-z)}{1-z}\right]_+ +\left[\frac{3}{2}c_{3\,q\bar{q}}^{\mathrm{PIM}}c_{2\,q\bar{q}}^{\mathrm{PIM}}-\frac{\beta_0}{4}c_{3\,q\bar{q}}^{\mathrm{PIM}}\right]\left[\frac{\ln^2(1-z)}{1-z}\right]_+\\
&+\left[c_{3\,q\bar{q}}^{\mathrm{PIM}}c_{1\,q\bar{q}}^{\mathrm{PIM}}+(c_{2\,q\bar{q}}^{\mathrm{PIM}})^2-\zeta_2(c_{3\,q\bar{q}}^{\mathrm{PIM}})^2-\frac{\beta_0}{2}T_{2\,q\bar{q}}^{\mathrm{PIM}}+\frac{\beta_0}{4}c_{3\,q\bar{q}}^{\mathrm{PIM}}\ln\left(\frac{\mu_R^2}{s}\right)+2C_F K+8\frac{C_F}{C_A}\ln^2\left(\frac{u_1}{t_1}\right)\right]\left[\frac{\ln(1-z)}{1-z}\right]_+\\
&+\left[c_{2\,q\bar{q}}^{\mathrm{PIM}}c_{1\,q\bar{q}}^{\mathrm{PIM}}-\zeta_2 c_{2\,q\bar{q}}^{\mathrm{PIM}}c_{3\,q\bar{q}}^{\mathrm{PIM}}+\zeta_3(c_{3\,q\bar{q}}^{\mathrm{PIM}})^2-\frac{\beta_0}{2}T_{1\,q\bar{q}}^{\mathrm{PIM}}+\frac{\beta_0}{4}c_{2\,q\bar{q}}^{\mathrm{PIM}}\ln\left(\frac{\mu_R^2}{s}\right)+\mathcal{G}_{q\bar{q}}^{(2)}+C_F\frac{\beta_0}{4}\ln^2\left(\frac{\mu_F^2}{s}\right)\right.\\
&\left.-C_F K\ln\left(\frac{\mu_F^2}{s}\right)\right]\left[\frac{1}{1-z}\right]_+ +R_{q\bar{q}}^{\mathrm{PIM}}\delta(1-z)\Bigg\}.
\end{aligned} \tag{3.19}$$

To NNLL, the results in Eq. (3.19) are identical to the sum of Eqs. (B17) and (B18) of Ref. [3]. The scale-independent terms multiplying $[1/(1-z)]_+$ are the new NNNLL contribution to $f_{q\bar{q}}^{(2,0)}$ in PIM kinematics.

Again, only certain terms in $R_{q\bar{q}}^{\mathrm{PIM}}$ that can be determined exactly are included. The contributions to the $f_{q\bar{q}}^{(2,r)}$ scaling functions are given below. The terms multiplying $\delta(1-z)$ that involve the factorization and renormalization scales are

$$\begin{aligned}
F_{q\bar{q}}^{B_\mathrm{PIM}}\frac{\alpha_s^2(\mu_R^2)}{\pi^2}\Bigg[&\ln^2\left(\frac{\mu_F^2}{m^2}\right)\left\{\frac{9}{8}C_F^2-2\zeta_2 C_F^2+\frac{3}{16}C_F\beta_0\right\}-\frac{9}{8}\beta_0 C_F\ln\left(\frac{\mu_F^2}{m^2}\right)\ln\left(\frac{\mu_R^2}{m^2}\right)+\frac{3\beta_0^2}{16}\ln^2\left(\frac{\mu_R^2}{m^2}\right)\\
&+\ln\left(\frac{\mu_F^2}{m^2}\right)\left\{\frac{9}{4}C_F^2\ln\left(\frac{m^2}{s}\right)-\frac{3}{2}C_F\left[T_{1\,q\bar{q}}^{\mathrm{PIM}}+\frac{\beta_0}{2}\ln\left(\frac{m^2}{s}\right)\right]+2C_F\zeta_2\left[T_{2\,q\bar{q}}^{\mathrm{PIM}}-2C_F\ln\left(\frac{m^2}{s}\right)\right]-8C_F^2\zeta_3-2\gamma'^{(2)}_{q/q}\right\}\\
&+\ln\left(\frac{\mu_R^2}{m^2}\right)\left\{\frac{3\beta_0}{4}\left[-\frac{3}{2}C_F\ln\left(\frac{m^2}{s}\right)+\frac{\beta_0}{2}\ln\left(\frac{m^2}{s}\right)+T_{1\,q\bar{q}}^{\mathrm{PIM}}\right]+\frac{\beta_1}{8}\right\}\Bigg].
\end{aligned} \tag{3.20}$$

The contributions multiplying quadratic powers of $\ln(\mu^2/m^2)$ are proportional to $f_{q\bar{q}}^{(2,2)}$ while those linear in $\ln(\mu^2/m^2)$ are the new NNNLL contributions proportional to $f_{q\bar{q}}^{(2,1)}$ in PIM kinematics.

The terms multiplying $\delta(1-z)$ that arise from inversion and do not involve the factorization and renormalization scales are given by

$$\begin{aligned}
F_{q\bar{q}}^{B_\mathrm{PIM}}\frac{\alpha_s^2(\mu_R^2)}{\pi^2}\Bigg\{&-\frac{\zeta_2}{2}\left[T_{2\,q\bar{q}}^{\mathrm{PIM}}-2C_F\ln\left(\frac{m^2}{s}\right)\right]^2+\frac{1}{4}\zeta_2^2(c_{3\,q\bar{q}}^{\mathrm{PIM}})^2+\zeta_3 c_{3\,q\bar{q}}^{\mathrm{PIM}}\left[T_{2\,q\bar{q}}^{\mathrm{PIM}}-2C_F\ln\left(\frac{m^2}{s}\right)\right]\\
&-\frac{3}{4}\zeta_4(c_{3\,q\bar{q}}^{\mathrm{PIM}})^2-4\zeta_2\frac{C_F}{C_A}\ln^2\left(\frac{u_1}{t_1}\right)\Bigg\}.
\end{aligned} \tag{3.21}$$

These are the new virtual ζ contributions proportional to $f_{q\bar{q}}^{(2,0)}$ in PIM kinematics.

IV. NNLO SOFT CORRECTIONS TO $gg \rightarrow t\bar{t}$

A. The $gg \rightarrow t\bar{t}$ channel in 1PI kinematics

We now turn to the gg channel. We write the $\overline{\rm MS}$ NLO soft-plus-virtual corrections for $gg \rightarrow t\bar{t}$ in 1PI kinematics as

$$s^2 \frac{d^2\hat{\sigma}^{(1)\ \rm 1PI}_{gg}}{dt_1\, du_1} = F^{B\ \rm 1PI}_{gg} \frac{\alpha_s(\mu_R^2)}{\pi} \left\{ c^{\rm 1PI}_{3\ gg} \left[\frac{\ln(s_4/m^2)}{s_4}\right]_+ + c^{\rm 1PI}_{2\ gg}\left[\frac{1}{s_4}\right]_+ + c^{\rm 1PI}_{1\ gg}\delta(s_4)\right\} + \frac{\alpha_s^3(\mu_R^2)}{\pi}\left[A^c_{gg}\left[\frac{1}{s_4}\right]_+ + T^{c\,\rm 1PI}_{1\ gg}\delta(s_4)\right]. \tag{4.1}$$

The Born term is given by

$$F^{B\ \rm 1PI}_{gg} = 2\pi\alpha_s^2(\mu_R^2) K_{gg} N_c C_F \left[C_F - C_A \frac{t_1 u_1}{s^2}\right] B_{\rm QED}, \tag{4.2}$$

where $K_{gg} = (N_c^2-1)^{-2}$ is a color average factor and

$$B_{\rm QED} = \frac{t_1}{u_1} + \frac{u_1}{t_1} + \frac{4m^2 s}{t_1 u_1}\left(1 - \frac{m^2 s}{t_1 u_1}\right). \tag{4.3}$$

Equation (4.1), in the notation of Ref. [12], is identical to Eq. (B10) of Ref. [3]. Note that because of the complex color flow in the gg channel, entering at NLL, only some of the soft and virtual terms are proportional to the Born term. At NLO, the rest are included in

$$A^c_{gg} = \pi K_{gg} B_{\rm QED}(N_c^2-1)\left\{ N_c\left(1 - \frac{2t_1u_1}{s^2}\right) \times \left[\left(-C_F + \frac{C_A}{2}\right)({\rm Re}\, L_\beta + 1) + \frac{N_c}{2} + \frac{N_c}{2}\ln\left(\frac{t_1u_1}{m^2 s}\right)\right] + \frac{1}{N_c}(C_F - C_A)({\rm Re}\, L_\beta + 1) - \ln\left(\frac{t_1 u_1}{m^2 s}\right) + \frac{N_c^2}{2}\frac{(t_1^2 - u_1^2)}{s^2}\ln\left(\frac{u_1}{t_1}\right)\right\} \tag{4.4}$$

and

$$T^{c\,\rm 1PI}_{1\ gg} = \frac{\sigma^{(1)\rm S+V1PI}_{gg\,\delta}}{\alpha_s^3/\pi} \tag{4.5}$$

where $\sigma^{(1)\rm S+V1PI}_{gg\,\delta}$ denotes the scale-independent $\delta(s_4)$ terms in the NLO cross section. These terms are given by Eq. (6.19) in Ref. [15]. We also define $c^{\rm 1PI}_{3\ gg} = 4C_A$,

$$c^{\rm 1PI}_{2\ gg} = -2C_A - 2C_A \ln\left(\frac{t_1u_1}{m^4}\right) - 2C_A\ln\left(\frac{\mu_F^2}{s}\right) \equiv T^{\rm 1PI}_{2\ gg} - 2C_A \ln\left(\frac{\mu_F^2}{s}\right), \tag{4.6}$$

$$c^{\rm 1PI}_{1\ gg} = \left[C_A \ln\left(\frac{t_1u_1}{m^4}\right) - \frac{\beta_0}{2}\right]\ln\left(\frac{\mu_F^2}{s}\right) + \frac{\beta_0}{2}\ln\left(\frac{\mu_R^2}{s}\right). \tag{4.7}$$

The NNLO soft-plus-virtual corrections, including the new subleading terms, in 1PI kinematics are

$$s^2\frac{d^2\hat{\sigma}_{gg}^{(2)\ \rm 1PI}}{dt_1\,du_1} = F^{B\ \rm 1PI}_{gg}\frac{\alpha_s^2(\mu_R^2)}{\pi^2}\left\{\frac{1}{2}(c^{\rm 1PI}_{3\ gg})^2\left[\frac{\ln^3(s_4/m^2)}{s_4}\right]_+ + \left[\frac{3}{2}c^{\rm 1PI}_{3\ gg}c^{\rm 1PI}_{2\ gg} - \frac{\beta_0}{4}c^{\rm 1PI}_{3\ gg}\right]\left[\frac{\ln^2(s_4/m^2)}{s_4}\right]_+ \right.$$
$$+ \left[c^{\rm 1PI}_{3\ gg}c^{\rm 1PI}_{1\ gg} + (c^{\rm 1PI}_{2\ gg})^2 - \zeta_2 (c^{\rm 1PI}_{3\ gg})^2 - \frac{\beta_0}{2}T^{\rm 1PI}_{2\ gg} + \frac{\beta_0}{4}c^{\rm 1PI}_{3\ gg}\ln\left(\frac{\mu_R^2}{s}\right) + 2C_A K\right]\left[\frac{\ln(s_4/m^2)}{s_4}\right]_+$$
$$+ \left[c^{\rm 1PI}_{2\ gg}c^{\rm 1PI}_{1\ gg} - \zeta_2 c^{\rm 1PI}_{2\ gg}c^{\rm 1PI}_{3\ gg} + \zeta_3 (c^{\rm 1PI}_{3\ gg})^2 + \frac{\beta_0}{4}c^{\rm 1PI}_{2\ gg}\ln\left(\frac{\mu_R^2}{s}\right)\right.$$
$$\left.\left. + \mathcal{G}^{(2)}_{gg} + C_A\frac{\beta_0}{4}\ln^2\left(\frac{\mu_F^2}{s}\right) - C_A K \ln\left(\frac{\mu_F^2}{s}\right) - C_A K\ln\left(\frac{t_1u_1}{m^4}\right)\right]\left[\frac{1}{s_4}\right]_+ + R^{\rm 1PI}_{gg}\delta(s_4)\right\}$$
$$+ \frac{\alpha_s^4(\mu_R^2)}{\pi^2}\left\{\frac{3}{2}c^{\rm 1PI}_{3\ gg}A^c_{gg}\left[\frac{\ln^2(s_4/m^2)}{s_4}\right]_+ + \left[\left(2c^{\rm 1PI}_{2\ gg} - \frac{\beta_0}{2}\right)A^c_{gg} + c^{\rm 1PI}_{3\ gg}T^{c\,\rm 1PI}_{1\ gg} + F^c_{gg}\right]\left[\frac{\ln(s_4/m^2)}{s_4}\right]_+\right.$$
$$\left. + \left[\left(c^{\rm 1PI}_{1\ gg} - \zeta_2 c^{\rm 1PI}_{3\ gg} + \frac{\beta_0}{4}\ln\left(\frac{\mu_R^2}{s}\right)\right)A^c_{gg} + \left(c^{\rm 1PI}_{2\ gg} - \frac{\beta_0}{2}\right)T^{c\,\rm 1PI}_{1\ gg} + F^c_{gg}\ln\left(\frac{m^2}{s}\right)\right]\left[\frac{1}{s_4}\right]_+ + R^{c\,\rm 1PI}_{gg}\delta(s_4)\right\}, \tag{4.8}$$

where

$$F^c_{gg}=\frac{\pi}{2}K_{gg}B_{\rm QED}(N_c^2-1)$$
$$\times\left\{2\ln\left(\frac{u_1}{t_1}\right)\frac{(t_1^2-u_1^2)}{s^2}[4\Gamma_{11}^{gg}+2(N_c^2-2)\Gamma_{22}^{gg}]\right.$$
$$+\left(1-\frac{2t_1u_1}{s^2}\right)N_c\left[4(\Gamma_{22}^{gg})^2+(N_c^2+4)\ln^2\left(\frac{u_1}{t_1}\right)\right]$$
$$\left.+\frac{4}{N_c}[(\Gamma_{11}^{gg})^2-2(\Gamma_{22}^{gg})^2]-2N_c\ln^2\left(\frac{u_1}{t_1}\right)\right\}, \tag{4.9}$$

with

$$\Gamma_{11}^{gg}\equiv-C_F(L'_\beta+1)+C_A\,,$$
$$\Gamma_{22}^{gg}\equiv-C_F(L'_\beta+1)+\frac{C_A}{2}\left[2+\ln\left(\frac{t_1u_1}{m^2s}\right)+L'_\beta\right]. \tag{4.10}$$

Here

$$\mathcal{G}^{(2)}_{gg}=C_A^2\left(\frac{7}{2}\zeta_3+\frac{22}{3}\zeta_2-\frac{41}{108}\right)+n_fC_A\left(-\frac{4}{3}\zeta_2-\frac{5}{54}\right) \tag{4.11}$$

denotes a set of universal two-loop contributions for processes with gg initial states [12]. Process-dependent two-loop corrections [14] are not included in $\mathcal{G}^{(2)}_{gg}$. To NNLL, the results in Eq. (4.8) are identical to the sum of Eqs. (B11) and (B12) of Ref. [3]. The scale-independent terms multiplying $[1/s_4]_+$ are the new NNNLL contribution to $f^{(2,0)}_{gg}$ in 1PI kinematics.

The complex color flow now gives us two contributions to the virtual corrections, $R^{1\rm PI}_{\underline{gg}}$, proportional to the Born term, and $R^{c1\rm PI}_{gg}$. As for the qq channel, we include only certain terms that can be determined exactly. The terms multiplying $\delta(s_4)$ involving the factorization and renormalization scales are

$$F^B_{gg}{}^{1\rm PI}\frac{\alpha_s^2(\mu_R^2)}{\pi^2}\left[\ln^2\left(\frac{\mu_F^2}{m^2}\right)\left\{\frac{C_A^2}{2}\ln^2\left(\frac{t_1u_1}{m^4}\right)-\frac{5\beta_0}{8}C_A\ln\left(\frac{t_1u_1}{m^4}\right)+\frac{3\beta_0^2}{16}-2\zeta_2C_A^2\right\}\right.$$
$$+\ln\left(\frac{\mu_F^2}{m^2}\right)\ln\left(\frac{\mu_R^2}{m^2}\right)\frac{3\beta_0}{4}\left[C_A\ln\left(\frac{t_1u_1}{m^4}\right)-\frac{\beta_0}{2}\right]+\ln^2\left(\frac{\mu_R^2}{m^2}\right)\frac{3\beta_0^2}{16}$$
$$+\ln\left(\frac{\mu_F^2}{m^2}\right)\left\{C_A^2\ln^2\left(\frac{t_1u_1}{m^4}\right)\ln\left(\frac{m^2}{s}\right)-\frac{\beta_0}{2}C_A\ln\left(\frac{t_1u_1}{m^4}\right)\ln\left(\frac{m^2}{s}\right)+2C_A\zeta_2\left[T^{1\rm PI}_{2\ gg}-2C_A\ln\left(\frac{m^2}{s}\right)\right]\right.$$
$$\left.\left.-8C_A^2\zeta_3+C_A\frac{K}{2}\ln\left(\frac{t_1u_1}{m^4}\right)-2\gamma'^{(2)}_{g/g}\right\}+\ln\left(\frac{\mu_R^2}{m^2}\right)\left\{\frac{3\beta_0}{4}C_A\ln\left(\frac{t_1u_1}{m^4}\right)\ln\left(\frac{m^2}{s}\right)+\frac{\beta_1}{8}\right\}\right]$$
$$+\frac{\alpha_s^4(\mu_R^2)}{\pi^2}\left\{\left[2C_A\zeta_2A^c_{gg}+\left(C_A\ln\left(\frac{t_1u_1}{m^4}\right)-\frac{\beta_0}{2}\right)T^{c1\rm PI}_{1\ gg}\right]\ln\left(\frac{\mu_F^2}{m^2}\right)+\frac{3\beta_0}{4}T^{c1\rm PI}_{1\ gg}\ln\left(\frac{\mu_R^2}{m^2}\right)\right\} \tag{4.12}$$

where

$$\gamma'^{(2)}_{g/g}=C_A^2\left(\frac{2}{3}+\frac{3}{4}\zeta_3\right)-n_f\left(\frac{C_F}{8}+\frac{C_A}{6}\right). \tag{4.13}$$

The contributions multiplying quadratic powers of $\ln(\mu^2/m^2)$ are proportional to $f^{(2,2)}_{gg}$ at NNLL while those linear in $\ln(\mu^2/m^2)$ are the new NNNLL contributions proportional to $f^{(2,1)}_{gg}$ in 1PI kinematics.

The terms multiplying $\delta(s_4)$ that arise from inversion and do not involve the factorization and renormalization scales are

$$F^B_{gg}{}^{1\rm PI}\frac{\alpha_s^2(\mu_R^2)}{\pi^2}\left\{-\frac{\zeta_2}{2}\left[T^{1\rm PI}_{2\ gg}-2C_A\ln\left(\frac{m^2}{s}\right)\right]^2+\frac{1}{4}\zeta_2^2(c^{1\rm PI}_{3\ gg})^2\right.$$
$$\left.+\zeta_3c^{1\rm PI}_{3\ gg}\left[T^{1\rm PI}_{2\ gg}-2C_A\ln\left(\frac{m^2}{s}\right)\right]-\frac{3}{4}\zeta_4(c^{1\rm PI}_{3\ gg})^2\right\}$$
$$+\frac{\alpha_s^4(\mu_R^2)}{\pi^2}\left\{\left[\zeta_3c^{1\rm PI}_{3\ gg}-\zeta_2\left(T^{1\rm PI}_{2\ gg}-2C_A\ln\left(\frac{m^2}{s}\right)\right)\right]A^c_{gg}\right.$$
$$\left.-\frac{\zeta_2}{2}F^c_{gg}\right\}. \tag{4.14}$$

These are the subleading virtual ζ contributions proportional to $f_{gg}^{(2,0)}$.

B. The $gg \to t\bar{t}$ channel in PIM kinematics

We continue our study of subleading terms in the gg channel by writing the $\overline{\rm MS}$ NLO soft-plus-virtual corrections for $gg \to t\bar{t}$ in PIM kinematics as

$$s\frac{d^2\hat{\sigma}_{gg}^{(1)\ \rm PIM}}{dM^2 d\cos\theta} = F_{gg}^{B\ \rm PIM}\frac{\alpha_s(\mu_R^2)}{\pi}\left\{c_{3\ gg}^{\rm PIM}\left[\frac{\ln(1-z)}{1-z}\right]_+ + c_{2\ gg}^{\rm PIM}\left[\frac{1}{1-z}\right]_+ + c_{1\ gg}^{\rm PIM}\delta(1-z)\right\} + \frac{\alpha_s^3(\mu_R^2)}{\pi}\left[A_{gg}^c\left[\frac{1}{1-z}\right]_+ + T_{1\ gg}^{c\rm PIM}\delta(1-z)\right]. \tag{4.15}$$

Here the Born term is

$$F_{gg}^{B\ \rm PIM} = \frac{\beta}{2s}F_{gg}^{B\ \rm 1PI}\Big|_{\rm PIM}. \tag{4.16}$$

Equation (4.15), in the notation of Ref. [12], is identical to Eq. (B24) of Ref. [3]. In addition, $c_{3\ gg}^{\rm PIM} = 4C_A$,

$$c_{2\ gg}^{\rm PIM} = -2C_A - 2C_A\ln\left(\frac{\mu_F^2}{s}\right) \equiv T_{2\ gg}^{\rm PIM} - 2C_A\ln\left(\frac{\mu_F^2}{s}\right), \tag{4.17}$$

$$c_{1\ gg}^{\rm PIM} = -\frac{\beta_0}{2}\ln\left(\frac{\mu_F^2}{s}\right) + \frac{\beta_0}{2}\ln\left(\frac{\mu_R^2}{s}\right). \tag{4.18}$$

Finally,

$$T_{1\ gg}^{\rm PIM} = 2T_{1\ gg}^{\rm 1PI}\Big|_{\rm PIM} + \frac{1}{\alpha_s^2}s\frac{d^2\sigma'^{(1)\ \rm S+MF}_{gg}}{dM^2 d\cos\theta} - \frac{1}{\alpha_s^2}\frac{\beta}{s}s^2\frac{d^2\sigma'^{(1)\ \rm S+MF}_{gg}}{dt_1 du_1}\Bigg|_{\rm PIM}. \tag{4.19}$$

Here $\sigma'^{(1)\ \rm S+MF}_{gg}$ denotes the soft and mass factorization subtraction terms calculated in Ref. [3]. The prime indicates that we drop the overall $\delta(1-z)$ or $\delta(s_4)$ coefficients from the expressions in Eqs. (82), (A10), and (A11) of Ref. [3].

The NNLO soft-plus-virtual corrections in PIM kinematics, including the new subleading contributions, are

$$\begin{aligned}
s\frac{d^2\hat{\sigma}_{gg}^{(2)\ \rm PIM}}{dM^2 d\cos\theta} = F_{gg}^{B\ \rm PIM}\frac{\alpha_s^2(\mu_R^2)}{\pi^2}\Bigg\{&\frac{1}{2}(c_{3\ gg}^{\rm PIM})^2\left[\frac{\ln^3(1-z)}{1-z}\right]_+ + \left[\frac{3}{2}c_{3\ gg}^{\rm PIM}c_{2\ gg}^{\rm PIM} - \frac{\beta_0}{4}c_{3\ gg}^{\rm PIM}\right]\left[\frac{\ln^2(1-z)}{1-z}\right]_+ \\
&+\left[c_{3\ gg}^{\rm PIM}c_{1\ gg}^{\rm PIM} + (c_{2\ gg}^{\rm PIM})^2 - \zeta_2(c_{3\ gg}^{\rm PIM})^2 - \frac{\beta_0}{2}T_{2\ gg}^{\rm PIM} + \frac{\beta_0}{4}c_{3\ gg}^{\rm PIM}\ln\left(\frac{\mu_R^2}{s}\right) + 2C_A K\right]\left[\frac{\ln(1-z)}{1-z}\right]_+ \\
&+\left[c_{2\ gg}^{\rm PIM}c_{1\ gg}^{\rm PIM} - \zeta_2 c_{2\ gg}^{\rm PIM}c_{3\ gg}^{\rm PIM} + \zeta_3(c_{3\ gg}^{\rm PIM})^2 + \frac{\beta_0}{4}c_{2\ gg}^{\rm PIM}\ln\left(\frac{\mu_R^2}{s}\right) + \mathcal{G}_{gg}^{(2)}\right. \\
&\left.+C_A\frac{\beta_0}{4}\ln^2\left(\frac{\mu_F^2}{s}\right) - C_A K\ln\left(\frac{\mu_F^2}{s}\right)\right]\left[\frac{1}{1-z}\right]_+ + R_{gg}^{\rm PIM}\delta(1-z)\Bigg\} \\
&+\frac{\alpha_s^4(\mu_R^2)}{\pi^2}\Bigg\{\frac{3}{2}c_{3\ gg}^{\rm PIM}A'^c_{gg}\left[\frac{\ln^2(1-z)}{1-z}\right]_+ + \left[\left(2c_{2\ gg}^{\rm PIM} - \frac{\beta_0}{2}\right)A'^c_{gg} + c_{3\ gg}^{\rm PIM}T_{1\ gg}^{c\rm PIM} + F'^c_{gg}\right]\left[\frac{\ln(1-z)}{1-z}\right]_+ \\
&+\left[\left(c_{1\ gg}^{\rm PIM} - \zeta_2 c_{3\ gg}^{\rm PIM} + \frac{\beta_0}{4}\ln\left(\frac{\mu_R^2}{s}\right)\right)A'^c_{gg} + \left(c_{2\ gg}^{\rm PIM} - \frac{\beta_0}{2}\right)T_{1\ gg}^{c\rm PIM}\right]\left[\frac{1}{1-z}\right]_+ + R_{gg}^{c\rm PIM}\delta(1-z)\Bigg\},
\end{aligned} \tag{4.20}$$

with

$$A'^c_{gg} = \frac{\beta}{2s}A_{gg}^c, \quad F'^c_{gg} = \frac{\beta}{2s}F_{gg}^c, \tag{4.21}$$

where A_{gg}^c and F_{gg}^c are the 1PI functions given in the previous subsection. To NNLL, the results in Eq. (4.20) are identical to the sum of Eqs. (B25) and (B26) of Ref. [3]. The scale-independent terms multiplying $[1/(1-z)]_+$ are the new NNNLL contribution proportional to $f_{gg}^{(2,0)}$ in PIM kinematics.

Neither of the virtual corrections, $R_{gg}^{\rm PIM}$ or $R_{gg}^{c\rm PIM}$, are fully known. We keep only those terms that are determined exactly. The terms multiplying $\delta(1-z)$ that involve the factorization and renormalization scales are

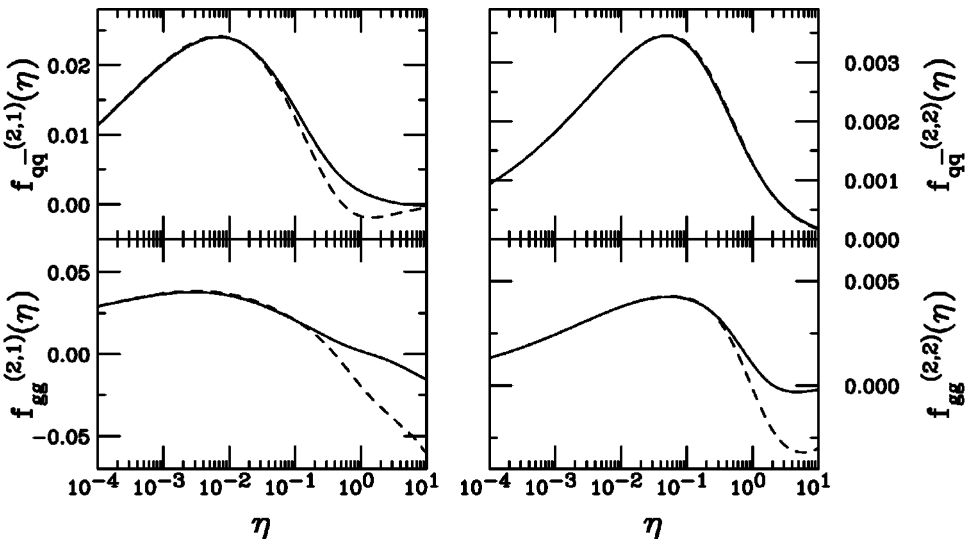

FIG. 1. The $\overline{\rm MS}$ scheme scaling functions multiplying the scale-dependent logarithms, $f_{ij}^{(2,1)}$ (left-hand side) and $f_{ij}^{(2,2)}$ (right-hand side). The upper plots are for the $q\bar q$ channel while the lower plots are for the gg channel. The solid curves are for 1PI kinematics, the dashed for PIM kinematics.

$$F^{B\ \rm PIM}_{gg}\frac{\alpha_s^2(\mu_R^2)}{\pi^2}\left[\ln^2\left(\frac{\mu_F^2}{m^2}\right)\left\{\frac{3\beta_0^2}{16}-2\zeta_2C_A^2\right\}-\frac{3\beta_0^2}{8}\ln\left(\frac{\mu_F^2}{m^2}\right)\ln\left(\frac{\mu_R^2}{m^2}\right)+\frac{3\beta_0^2}{16}\ln^2\left(\frac{\mu_R^2}{m^2}\right)\right.$$
$$\left.+\ln\left(\frac{\mu_F^2}{m^2}\right)\left\{2C_A\zeta_2\left[T_{2\ gg}^{\rm PIM}-2C_A\ln\left(\frac{m^2}{s}\right)\right]-8C_A^2\zeta_3-2\gamma'^{(2)}_{g/g}\right\}+\frac{\beta_1}{8}\ln\left(\frac{\mu_R^2}{m^2}\right)\right]$$
$$+\frac{\alpha_s^4(\mu_R^2)}{\pi^2}\left\{\left[2C_A\zeta_2A'^{c}_{gg}-\frac{\beta_0}{2}T_{1\ gg}^{c\rm PIM}\right]\ln\left(\frac{\mu_F^2}{m^2}\right)+\frac{3\beta_0}{4}T_{1\ gg}^{c\rm PIM}\ln\left(\frac{\mu_R^2}{m^2}\right)\right\}. \tag{4.22}$$

The contributions multiplying quadratic powers of $\ln(\mu^2/m^2)$ are proportional to $f_{gg}^{(2,2)}$ at NNLL, given in Ref. [3], while those linear in $\ln(\mu^2/m^2)$ are the new NNNLL contributions proportional to $f_{gg}^{(2,1)}$ in PIM kinematics.

The terms multiplying $\delta(1-z)$ that arise from inversion and do not involve the factorization and renormalization scales are

$$F^{B\ \rm PIM}_{gg}\frac{\alpha_s^2(\mu_R^2)}{\pi^2}\left\{-\frac{\zeta_2}{2}\left[T_{2\ gg}^{\rm PIM}-2C_A\ln\left(\frac{m^2}{s}\right)\right]^2+\frac{1}{4}\zeta_2^2(c_{3\ gg}^{\rm PIM})^2\right.$$
$$\left.+\zeta_3c_{3\ gg}^{\rm PIM}\left[T_{2\ gg}^{\rm PIM}-2C_A\ln\left(\frac{m^2}{s}\right)\right]-\frac{3}{4}\zeta_4(c_{3\ gg}^{\rm PIM})^2\right\}$$
$$+\frac{\alpha_s^4(\mu_R^2)}{\pi^2}\left\{\left[\zeta_3c_{3\ gg}^{\rm PIM}-\zeta_2\left(T_{2\ gg}^{\rm PIM}-2C_A\ln\left(\frac{m^2}{s}\right)\right)\right]A'^{c}_{gg}\right.$$
$$\left.-\frac{\zeta_2}{2}F'^{c}_{gg}\right\}. \tag{4.23}$$

These are the new virtual corrections proportional to $f_{gg}^{(2,0)}$ in PIM kinematics.

V. PARTONIC CROSS SECTIONS

In this section, we present numerical results for the $f_{ij}^{(2,r)}$ scaling functions in the $q\bar q$ and gg channels. We give the complete soft-plus-virtual $f_{ij}^{(2,2)}$ (to NNLL) and $f_{ij}^{(2,1)}$ (to NNNLL) scaling functions and the partial results for $f_{ij}^{(2,0)}$ that include the soft NNNLL and the virtual ζ terms calculated in Secs. III and IV.

We begin with a comparison of the full soft-plus-virtual 1PI and PIM contributions to $f_{ij}^{(2,1)}$ and $f_{ij}^{(2,2)}$, shown in Fig. 1. The upper plots are for the $q\bar q$ channel. The left-hand side of Fig. 1 compares the NNNLL 1PI and PIM scaling functions for $f_{q\bar q}^{(2,1)}$. At low η, closer to partonic threshold, the agreement is very good, better than that obtained at NNLL in Ref. [3]. The agreement is also improved at large η. The right-hand side shows the $f_{q\bar q}^{(2,2)}$ scaling functions in both kinematics. The results for $f_{q\bar q}^{(2,2)}$ remain unchanged from those of Ref. [3]. The agreement of $f_{q\bar q}^{(2,2)}$ between the two kinematics choices is excellent—the results are virtually indistinguishable.

The lower plots of Fig. 1 show the corresponding scaling functions in the gg channel. The agreement of the NNNLL $f_{gg}^{(2,1)}$ scaling functions between the two kinematics choices is somewhat improved at high η compared to previous NNLL results [3]. We note that there is some ambiguity in the way that the expressions for the gg partonic cross sections can be written at threshold. We have investigated the effect of replacing $1-2t_1u_1/s^2$ with $(t_1^2+u_1^2)/s^2$ in Eq. (4.4), more consistent with the expressions in Ref. [15]. These two ex-

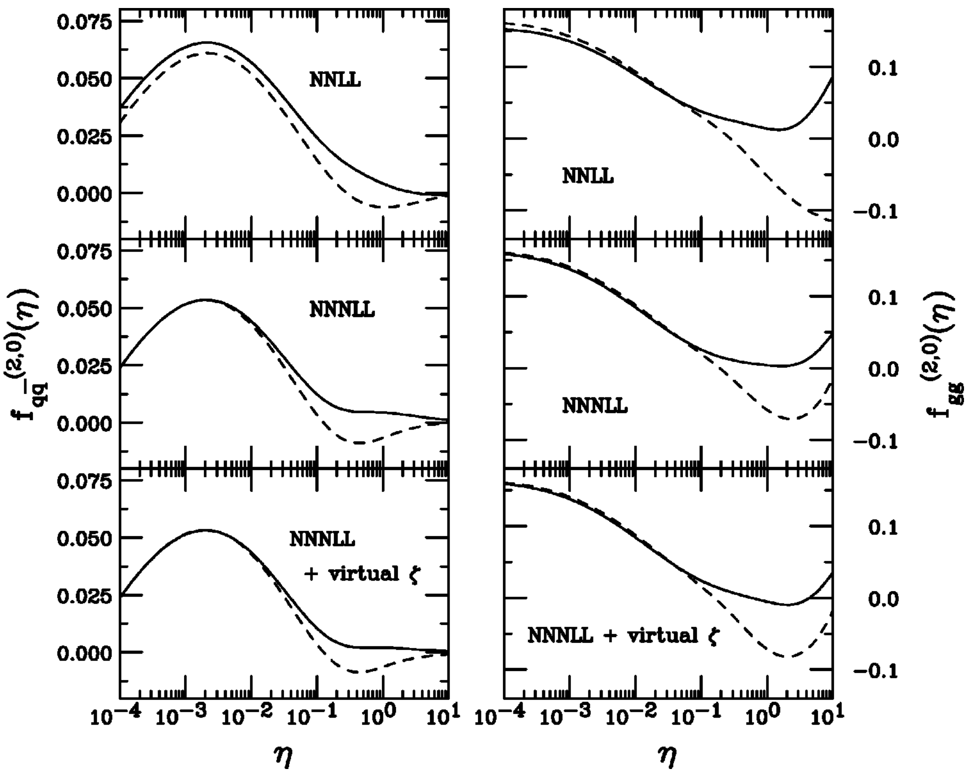

FIG. 2. The $f_{ij}^{(2,0)}$ scaling functions in the $\overline{\rm MS}$ scheme. The left-hand side shows the results for the $q\bar{q}$ channel while the right-hand side shows the results for the gg channel. The top plots show the NNLL result from Ref. [3]. The center plots give the results through NNNLL and the bottom plots give the results including the virtual ζ terms. The solid curves are for 1PI kinematics, the dashed for PIM kinematics.

pressions are equivalent at threshold, $s_4=0$ and $z=1$, but can differ at large η. Note that $f_{gg}^{(2,2)}$ is not affected by this replacement since there is no contribution from Eq. (4.4). The resulting differences in $f_{gg}^{(2,1)}$ are small, appearing only at $\eta>0.1$ where the agreement between the scaling functions in the two kinematics begins to diverge. The main effect of the second choice is to make the PIM result for $f_{gg}^{(2,1)}$ more negative at large η. We thus use the expressions as written in Sec. IV to be consistent with those of Ref. [3].

We now turn to the $f_{ij}^{(2,0)}$ scaling functions, the most important contributions at NNLO since they are independent of $\ln(\mu^2/m^2)$. We add the NNNLL terms, i.e. terms proportional to $[1/s_4]_+$ (1PI) and $[1/(1-z)]_+$ (PIM), to our previous NNLO-NNLL calculation. We also investigate the effect of keeping the virtual ζ terms resulting from the inversion from moment to momentum space. To demonstrate the effect of adding successive subleading contributions, in Fig. 2 we show the NNLL results in the upper plots, including the new NNNLL contributions alone in the middle plots, and adding the virtual ζ terms, Eqs. (3.13), (3.21), (4.14) and (4.23), in the lower plots.

We first discuss the results for the $q\bar{q}$ channel in the $\overline{\rm MS}$ scheme, shown on the left-hand side of Fig. 2. Note that to NNLL, the two kinematics choices give rather different results, even at low η. When the NNNLL contribution is added, both the 1PI and PIM results are reduced relative to the NNLL over all η. The agreement between the two kinematics is much improved up to $\eta>0.01$. Adding the virtual ζ terms resulting from inversion improves the agreement between the 1PI and PIM kinematics further for $0.01<\eta<0.1$. At $\eta>0.1$, the region where the parton luminosity peaks for $t\bar{t}$ production at the Tevatron, the additional virtual ζ terms provide a further small reduction. With the subleading terms, the 1PI result is smaller than previously but positive while the PIM result becomes more negative. However, on the whole, the subleading terms bring the 1PI and PIM results into better agreement over all η. The effect of the virtual ζ terms is numerically small. This small effect is in agreement with the arguments in Sec. III C of Ref. [2] concerning resummation prescriptions. There it was shown that when subleading terms from inversion are calculated exactly they do not have an unwarrantedly large effect on the numerical results.

A similar trend is seen for the gg channel on the right-hand side of Fig. 2. The agreement between the NNLL 1PI and PIM scaling functions at low η is significantly better than in the $q\bar{q}$ channel. This may perhaps be a consequence of the more complex color structure of the gg channel. Note however the significant divergence at large η. The 1PI NNLL result is large and positive while the PIM is large and negative. Again, inclusion of the subleading contributions improves agreement over all η. There is only a small improvement possible at low η. However, the improvement at larger η, $\eta>0.1$ is notable. The 1PI result with soft NNNLL plus virtual ζ terms is reduced by nearly a factor of two relative to the NNLL result at $\eta=10$. The difference between the NNNLL result with and without the virtual ζ terms is, however, also small in this channel. Likewise, the subleading terms stop and reverse the downward trend of the PIM scaling functions. The 1PI gg contribution will still be positive while the PIM will still be negative but the difference may not be as large as before. Using the alternate expression, $(t_1^2+u_1^2)/s^2$, in Eq. (4.4) does not significantly change the results, particularly for 1PI kinematics. The PIM

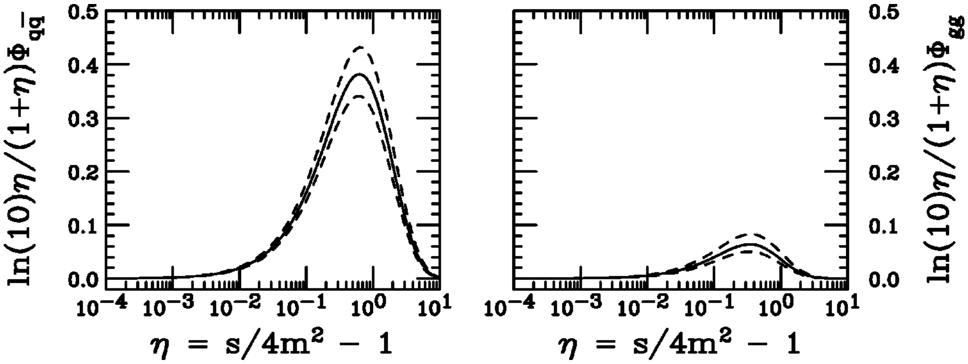

FIG. 3. The $q\bar{q}$ (left-hand side) and gg (right-hand side) parton luminosities in $p\bar{p}$ collisions at $\sqrt{S}=1.96$ TeV. The solid curves are calculated with $\mu=m=175$ GeV while the upper dashed curves are with $\mu=m/2$ and the lower dashed curves with $\mu=2m$.

result becomes slightly more negative at intermediate η, $\eta\approx 1$.

Finally we note that if we had kept only the ζ contributions in the $[1/s_4]_+$ and $[1/(1-z)]_+$ terms, the 1PI and PIM results would not have agreed near threshold. The full NNNLL result, given in Secs. III and IV, is required for the result to be independent of kinematics choice near threshold. This agreement also indicates that additional two-loop contributions not included in our expressions should be small.

We now turn to our calculations of the hadronic total cross sections and transverse momentum distributions.

VI. HADRONIC TOTAL CROSS SECTIONS AND p_T DISTRIBUTIONS

The inclusive hadronic cross section is obtained by convoluting the inclusive partonic cross sections with the parton luminosity, Φ_{ij}, defined as

$$\Phi_{ij}(\tau,\mu_F^2)=\tau\int_0^1 dx_1\int_0^1 dx_2\,\delta(x_1x_2-\tau)\times\phi_{i/h_1}(x_1,\mu_F^2)\,\phi_{j/h_2}(x_2,\mu_F^2), \tag{6.1}$$

where $\phi_{i/h}(x,\mu_F^2)$ is the density of partons of flavor i in hadron h carrying a fraction x of the initial hadron momentum, at factorization scale μ_F. Then

$$\sigma_{h_1h_2}(S,m^2)=\sum_{i,j=q,\bar{q},g}\int_{4m^2/S}^1\frac{d\tau}{\tau}\Phi_{ij}(\tau,\mu_F^2)\sigma_{ij}(\tau S,m^2,\mu_F^2)$$
$$=\sum_{i,j=q,\bar{q},g}\int_{-\infty}^{\log_{10}(S/4m^2-1)}d\log_{10}\eta\,\frac{\eta}{1+\eta}\times\ln(10)\Phi_{ij}(\eta,\mu_F^2)\sigma_{ij}(\eta,m^2,\mu_F^2) \tag{6.2}$$

where

$$\eta=\frac{s}{4m^2}-1=\frac{\tau S}{4m^2}-1, \tag{6.3}$$

and S is the hadronic Mandelstam invariant. Our investigations in Ref. [3] showed that the approximation should hold if the convolution of the parton densities is not very sensitive to the high η region.

We use the recent MRST2002 NNLO (approximate) parton densities [16] with an NNLO evaluation of α_s. The parton luminosities, weighted to emphasize the most important contributions to the hadronic cross sections, are shown for $\sqrt{S}=1.96$ TeV in Fig. 3. The $q\bar{q}$ luminosity is nearly 50% higher than the CTEQ5M [17] $q\bar{q}$ luminosity used in Ref. [3]. The gg luminosities for the two sets are rather similar. The peak of the luminosity is at $\eta<1$, but still in a regime where the 1PI and PIM results differ most. Fortunately the gg luminosity is small compared to the $q\bar{q}$ luminosity since the differences in the kinematics is largest in the gg channel.

Our calculations use the exact LO and NLO cross sections with the soft NNNLL and virtual ζ corrections to $f_{ij}^{(2,0)}$ and the full soft-plus-virtual scale-dependent terms $f_{ij}^{(2,1)}$ and

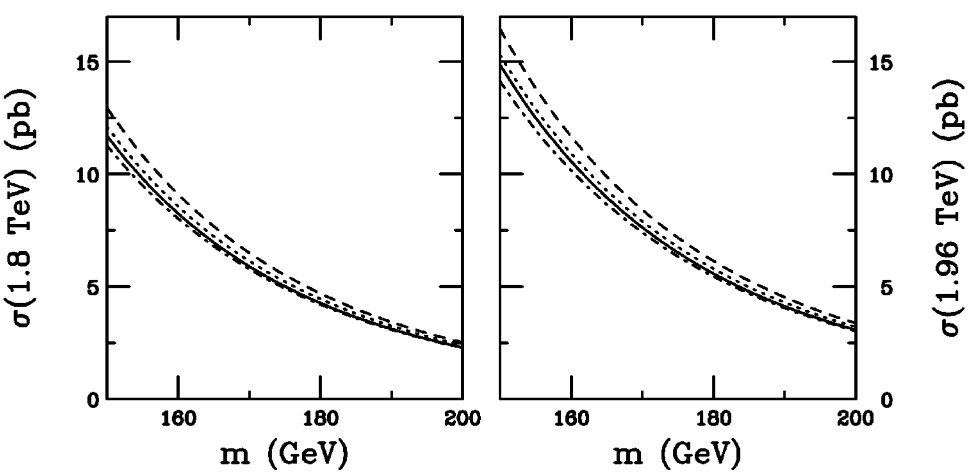

FIG. 4. The $t\bar{t}$ total cross sections in $p\bar{p}$ collisions at $\sqrt{S}=1.8$ TeV (left-hand side) and 1.96 TeV (right-hand side) as functions of m for $\mu=m$. The NLO (solid), and approximate NNLO-NNNLL$+\zeta$ 1PI (dashed), PIM (dot-dashed) and average (dotted) results are shown.

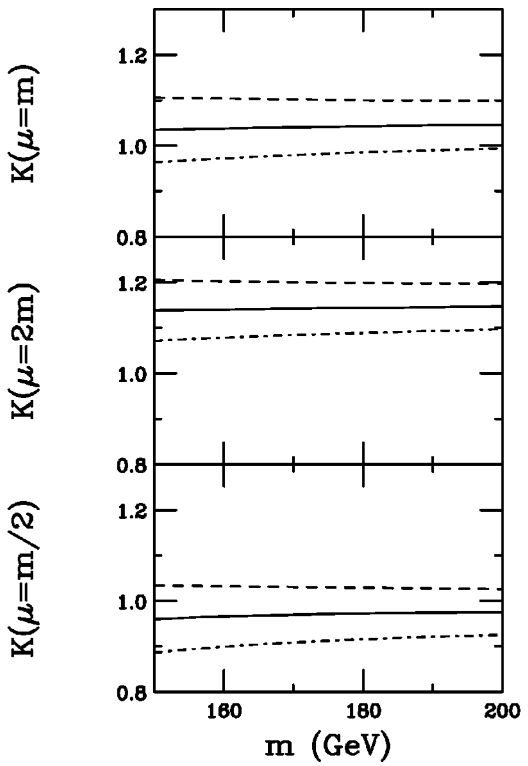

FIG. 5. The NNLO-NNNLL+ζ K factors at $\sqrt{S}=1.8$ TeV as functions of top quark mass in $p\bar{p}$ collisions with $\mu=m$ (upper), $\mu=2m$ (middle) and $\mu=m/2$ (lower). The curves show the ratio of the approximate NNLO-NNNLL+ζ 1PI (dashed), PIM (dot-dashed) and average (solid) cross sections to the NLO cross section.

$f_{ij}^{(2,2)}$ at NNLO given in Secs. III and IV. These cross sections are denoted NNLO-NNNLL+ζ in the following. To lessen the influence of the large η region where the threshold approximation does not hold so well, we multiply the NNLO scaling functions by a damping factor, $1/\sqrt{1+\eta}$, as in Ref. [3].

In Fig. 4, we present the NLO and approximate NNLO-NNNLL+ζ $t\bar{t}$ cross sections at $\sqrt{S}=1.8$ TeV (left-hand side) and 1.96 TeV (right-hand side) as functions of top quark mass for $\mu=m$. As expected from Fig. 3, the $q\bar{q}$ channel dominates for $p\bar{p}\rightarrow t\bar{t}$. The NNLO-NNNLL+$\zeta$ results are given in both 1PI and PIM kinematics. We also show the average of the two kinematics results, perhaps closer to the full NNLO result. Here the NNLO-NNNLL+ζ PIM cross section is slightly lower than the NLO cross section for all masses shown. In Ref. [3], the PIM cross section was a bit higher than the NLO. The reduction of the PIM $q\bar{q}$ result caused by the new subleading terms lowers the total PIM cross section. The NNLO-NNNLL+ζ 1PI cross section remains above the NLO for all m although reduced relative to the NNLO-NNLL cross section due to the subleading terms. The average of the two kinematics is just above the NLO cross sections for both energies.

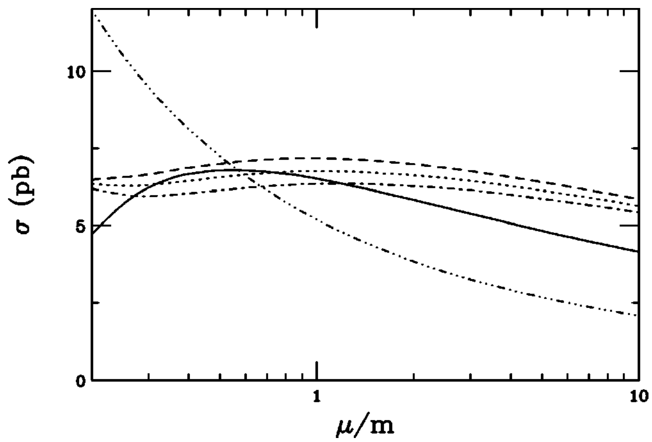

FIG. 7. The scale dependence of the $t\bar{t}$ total cross sections in $p\bar{p}$ collisions at $\sqrt{S}=1.96$ TeV as a function of μ/m. The LO (dot-dot-dot-dashed), NLO (solid), and approximate NNLO-NNNLL+ζ 1PI (dashed), PIM (dot-dashed) and average (dotted) results are shown.

Going to higher scales increases all the NNLO-NNNLL+ζ corrections so that both kinematics choices give cross sections larger than the NLO. On the other hand, at lower scales, the NNLO-NNNLL+ζ cross sections are reduced relative to NLO. The ratio of the NNLO-NNNLL+ζ cross sections to the NLO cross sections, the K factors, are shown in Fig. 5 as functions of mass for $\mu=m$ (upper plot), $2m$ (middle plot) and $m/2$ (lower plot) at $\sqrt{S}=1.8$ TeV. In keeping with the results in Fig. 4, when $\mu=m$, $K<1$ for PIM

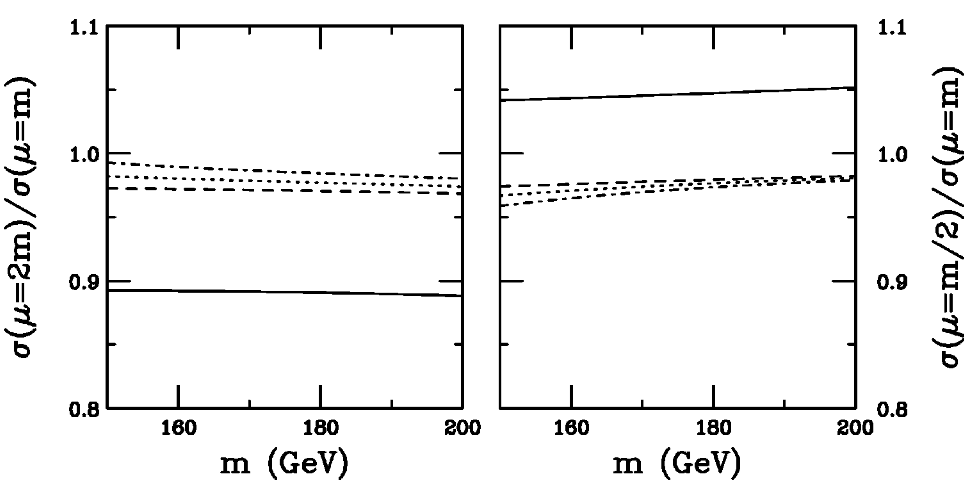

FIG. 6. The scale dependence of the $t\bar{t}$ total cross sections in $p\bar{p}$ collisions at $\sqrt{S}=1.8$ TeV as a function of top quark mass. The left-hand side shows the ratio $(\mu=2m)/(\mu=m)$ while the right-hand side gives the ratio for $(\mu=m/2)/(\mu=m)$. The NLO (solid), and approximate NNLO-NNNLL+ζ 1PI (dashed), PIM (dot-dashed) and average (dotted) results are shown.

TABLE I. The $\overline{\mathrm{MS}}$ top quark production cross section in $p\bar{p}$ collisions at the Tevatron for $m=175$ GeV. The exact NLO results and the approximate NNLO-NNNLL $+\zeta$ results are shown.

		σ (pb)					
		MRST2002 NNLO			CTEQ6M		
$\sqrt{S}$ (TeV)	Order	$\mu=m/2$	$\mu=m$	$\mu=2m$	$\mu=m/2$	$\mu=m$	$\mu=2m$
	NLO	5.24	5.01	4.46	5.27	5.06	4.51
1.8	NNLO-NNNLL $+\zeta$ 1PI	5.40	5.52	5.36	5.43	5.58	5.43
	NNLO-NNNLL $+\zeta$ PIM	4.78	4.92	4.85	4.76	4.94	4.89
	NLO	6.79	6.52	5.83	6.79	6.54	5.85
1.96	NNLO-NNNLL $+\zeta$ 1PI	7.00	7.17	6.99	7.01	7.21	7.04
	NNLO-NNNLL $+\zeta$ PIM	6.14	6.35	6.28	6.08	6.33	6.29

kinematics, >1 for 1PI and for the average. The K factors are larger for $\mu=2m$ and smaller for $\mu=m/2$. Note also that K is almost independent of m. The NLO/LO K factor, ~ 1.25 for $\mu=m$, 1.52 for $\mu=2m$ and 0.94 for $\mu=m/2$, is also essentially mass independent but typically larger than the NNLO-NNNLL $+\zeta$/NLO K factors shown here. Only the $\mu=m/2$ value of the NLO/LO K factor is similar to that of the NNLO-NNNLL $+\zeta$/NLO average K factor in Fig. 5. The small K factors, calculated with the MRST2002 NNLO parton distribution functions at each order, indicate good convergence. Even though the results are shown at $\sqrt{S}=1.8$ TeV, the K factors at $\sqrt{S}=1.96$ TeV are very similar.

We now examine the scale dependence in Fig. 6 as a function of top quark mass and in Fig. 7 as a function of μ/m with $m=175$ GeV. Figure 6 shows the ratio of the cross sections with $\mu=2m$ to $\mu=m$ on the left-hand side and the ratio for $\mu=m/2$ to $\mu=m$ on the right-hand side at both NLO and NNLO-NNNLL $+\zeta$ at $\sqrt{S}=1.8$ TeV. The ratios are nearly independent of mass at this energy. The scale dependence is reduced at NNLO-NNNLL $+\zeta$ relative to NLO. The NNLO-NNNLL $+\zeta$ results are very similar for the two ratios. In contrast, the LO scale dependence is much larger, $\sigma(\mu=2m)/\sigma(\mu=m)\approx 0.74$ and $\sigma(\mu=m/2)/\sigma(\mu=m)\approx 1.4$. The difference between the scale dependence at $\sqrt{S}=1.8$ TeV and 1.96 TeV is negligible.

We have also calculated the cross sections as functions of μ/m for $0.2<\mu/m<10$ at $\sqrt{S}=1.96$ TeV and $m=175$ GeV in Fig. 7. The NLO cross section is not as strong a function of μ/m as the LO cross section. In fact, it is seen to rise with μ/m and then turn over. The NNLO-NNNLL $+\zeta$ cross sections, however, exhibit even less dependence on μ/m, approaching the independence of scale corresponding to a true physical cross section. They change by less than 15% over the entire range of μ/m considered. The change in the NNLO-NNNLL $+\zeta$ cross sections through the range $m/2<\mu<2m$, normally displayed as a measure of uncertainty due to scale variation, is less than 3%. Note also that, at this energy, the absolute difference between the NNLO-NNNLL $+\zeta$ 1PI and PIM cross sections is also not large.

In Table I, we give the NLO, NNLO-NNNLL $+\zeta$ 1PI and PIM $t\bar{t}$ total cross sections at $\sqrt{S}=1.8$ and 1.96 TeV for $p\bar{p}$ interactions, corresponding to Tevatron runs I and II. The results are presented for $m=175$ GeV and $\mu=m/2$, m, and $2m$. We show the results of our calculations with the MRST2002 NNLO parton densities [16] and the three-loop α_s. We compare these with results of calculations with the CTEQ6M NLO parton densities [18] and the two-loop α_s. The results with the two different sets of parton densities are quite similar even though the densities are evaluated to different orders. Note that the NNLO-NNNLL $+\zeta$ scale dependence is negligible compared to the NLO scale dependence, as shown in Fig. 7. The kinematics dependence of the

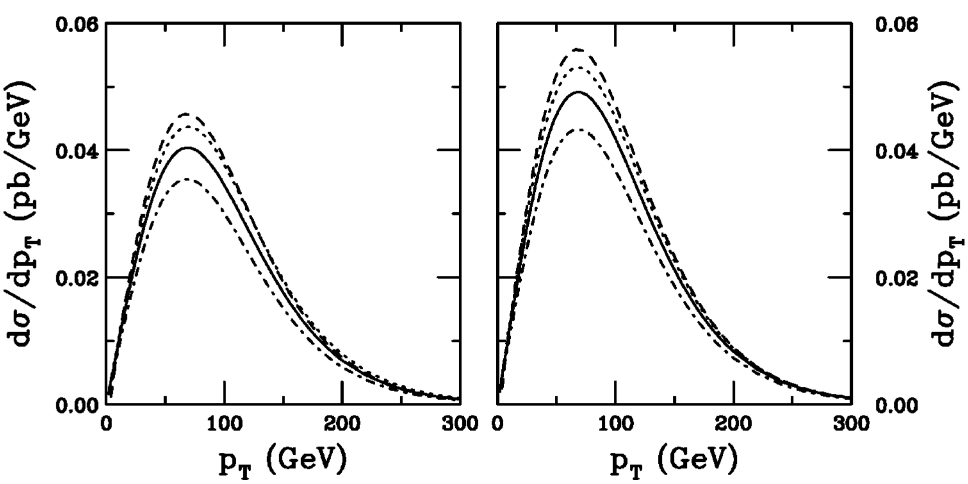

FIG. 8. The top quark transverse momentum distribution with $m=175$ GeV at $\sqrt{S}=1.8$ TeV (left) and 1.96 TeV (right). The NLO (solid: $\mu=m$; dotted: $\mu=m/2$; dot-dashed: $\mu=2m$), and approximate NNLO-NNNLL $+\zeta$ 1PI $\mu=m$ (dashed) results are shown.

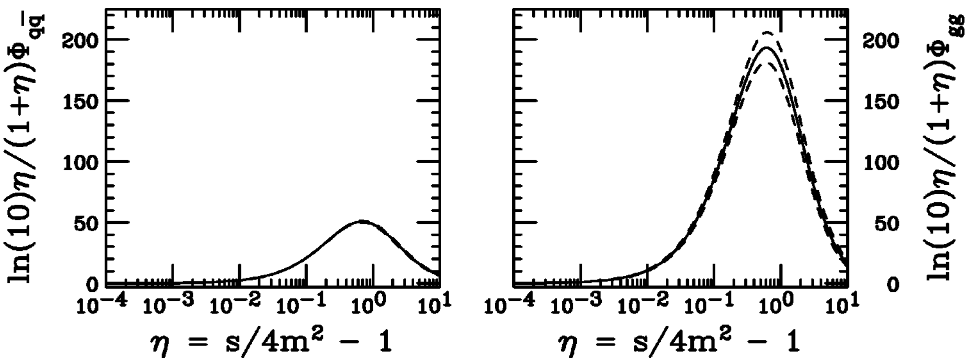

FIG. 9. The $q\bar{q}$ (left-hand side) and gg (right-hand side) parton luminosities in pp collisions at $\sqrt{S}=14$ TeV. The solid curves are calculated with $\mu=m=175$ GeV while the upper dashed curves are with $\mu=m/2$ and the lower dashed curves with $\mu=2m$.

NNLO-NNNLL$+\zeta$ cross sections thus remains the largest source of uncertainty. At $\sqrt{S}=1.8$ TeV, averaging over the 1PI and PIM NNLO-NNNLL$+\zeta$ results with the two sets of parton distributions at $\mu=m=175$ GeV, our best estimate for the cross section is 5.24 ± 0.31 pb where the quoted uncertainty is from the kinematics dependence. At $\sqrt{S}=1.96$ TeV our corresponding best estimate is 6.77 ± 0.42 pb.

We note that the cross sections presented in Table I are significantly lower than our previous estimates [2,3] at both NLO and NNLO. The difference at NLO is solely due to the new sets of parton densities used here, MRST2002 and CTEQ6M, relative to CTEQ5M in Refs. [2,3]. With these new densities, our NLO results, as well as the total NNLO-NNLL results derived in Ref. [3], are around 3% lower. The effect of the new densities on the NNLO corrections alone is even larger. The NNLO-NNLL 1PI corrections are smaller than our previous results [2,3] by 14% for $\mu=m$ and 18% for $\mu=2m$ with the MRST2002 NNLO densities. Most of this difference is due to the relative values of α_s between the two densities. In addition, the new subleading terms we have included here further reduce the magnitude of the NNLO corrections. The combined effect of the new parton densities and new subleading terms make our new estimates for the total NNLO-NNNLL$+\zeta$ $t\bar{t}$ cross section noticeably smaller.

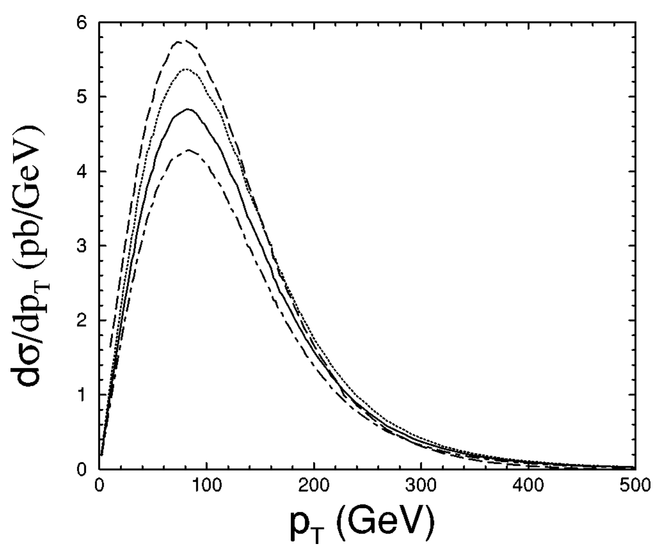

FIG. 10. The top quark transverse momentum distribution with $m=175$ GeV at $\sqrt{S}=14$ TeV. The NLO (solid: $\mu=m$; dotted: $\mu=m/2$; dot-dashed: $\mu=2m$), and approximate NNLO-NNNLL$+\zeta$ 1PI $\mu=m$ (dashed) results are shown.

In Fig. 8 we show the top quark transverse momentum distributions at $\sqrt{S}=1.8$ and 1.96 TeV. The NLO and NNLO-NNNLL$+\zeta$ 1PI results are shown using the MRST2002 NNLO densities. Details of the hadronic calculation of the p_T dependence are given in Appendix B of Ref. [2]. At NNLO-NNNLL$+\zeta$ we observe an enhancement of the NLO distribution with no significant change in shape. This pattern agrees with earlier, resummed, results on top transverse momentum and rapidity distributions [2,19].

Finally we discuss top production in pp collisions at the LHC. The weighted parton luminosities are shown in Fig. 9 for the maximum LHC pp energy, $\sqrt{S}=14$ TeV. The gg luminosity now dominates the $q\bar{q}$ by a factor of 4. The peak of the luminosity is still at $\eta\leqslant1$ so that this energy is not very far from partonic threshold. However, large uncertainties may be expected in the gg channel since the difference in the kinematics choice, largest in this channel, will be emphasized by the high gg luminosity.

Since the gg contribution dominates at high energy, the difference in the total cross sections between the two kinematics increases strongly with energy. The complex color structure of the gg channel may be better suited to 1PI kinematics and thus this kinematics choice could be more appropriate in processes where the gg channel dominates, see Ref. [11] for discussions of bottom and charm production. The NNLO-NNNLL$+\zeta$ 1PI scale dependence at high energy seems to support such a conclusion. At $\sqrt{S}=14$ TeV, the NNLO-NNNLL$+\zeta$ 1PI scale dependence is 4%, smaller than the 9% dependence of the NLO cross section, acceptable behavior, similar to that at the Tevatron. However, the NNLO-NNNLL$+\zeta$ gg PIM contribution is large and negative. The $q\bar{q}$ PIM contribution is also negative for $\mu\leqslant m$ albeit much smaller than the gg contribution. The NNLO-NNNLL$+\zeta$ PIM cross section is reduced by nearly a factor of two relative to the NLO. The scale dependence is similarly large. Thus we only provide NNLO-NNNLL$+\zeta$ 1PI results for the LHC. At $\sqrt{S}=14$ TeV with $m=175$ GeV and the MRST2002 NNLO parton densities, the NLO cross section is 808.8 pb for $\mu=m/2$, 794.1 pb for $\mu=m$, and 744.4 pb for $\mu=2m$. The corresponding NNLO-NNNLL$+\zeta$ 1PI cross sections are 845.2 pb for $\mu=m/2$, 872.8 pb for $\mu=m$, and 875.1 pb for $\mu=2m$. In Fig. 10 we show the NLO and NNLO-NNNLL$+\zeta$ 1PI top quark

p_T distributions at $\sqrt{S}=14$ TeV. Here also the NNLO-NNNLL $+\zeta$ corrections enhance the NLO result without a change in shape.

VII. CONCLUSIONS

In this paper we have calculated further soft NNLO corrections to the total top quark cross section and top transverse momentum distributions in hadron-hadron collisions. We have added new soft NNNLL terms and some virtual terms, including all soft-plus-virtual factorization and renormalization scale-dependent terms. We have found that these new subleading corrections greatly diminish the dependence of the cross section on the kinematics and on the factorization or renormalization scales. We have provided numerical results for the total cross section and top transverse momentum distributions for top quark production at the Tevatron, for both runs I and II, and at the LHC.

ACKNOWLEDGMENTS

The research of N.K. has been supported by a Marie Curie Fellowship of the European Community programme ''Improving Human Research Potential'' under contract number HPMF-CT-2001-01221. The research of R.V. is supported in part by the Division of Nuclear Physics of the Office of High Energy and Nuclear Physics of the U.S. Department of Energy under Contract No. DE-AC-03-76SF00098.

[1] CDF Collaboration, F. Abe *et al.*, Phys. Rev. Lett. **74**, 2626 (1995); D0 Collaboration, S. Abachi *et al.*, *ibid.* **74**, 2632 (1995).

[2] N. Kidonakis, Phys. Rev. D **64**, 014009 (2001).

[3] N. Kidonakis, E. Laenen, S. Moch, and R. Vogt, Phys. Rev. D **64**, 114001 (2001).

[4] N. Kidonakis and G. Sterman, Phys. Lett. B **387**, 867 (1996); Nucl. Phys. **B505**, 321 (1997).

[5] N. Kidonakis, G. Oderda, and G. Sterman, Nucl. Phys. **B525**, 299 (1998); **B531**, 365 (1998); N. Kidonakis, Int. J. Mod. Phys. A **15**, 1245 (2000).

[6] E. Laenen, G. Oderda, and G. Sterman, Phys. Lett. B **438**, 173 (1998).

[7] E. Laenen, J. Smith, and W.L. van Neerven, Nucl. Phys. **B369**, 543 (1992).

[8] E.L. Berger and H. Contopanagos, Phys. Lett. B **361**, 115 (1995).

[9] S. Catani, M.L. Mangano, P. Nason, and L. Trentadue, Phys. Lett. B **378**, 329 (1996).

[10] N. Kidonakis and R. Vogt, Phys. Rev. D **59**, 074014 (1999).

[11] N. Kidonakis, E. Laenen, S. Moch, and R. Vogt, Phys. Rev. D **67**, 074037 (2003); Nucl. Phys. **A715**, 549c (2003).

[12] N. Kidonakis, Int. J. Mod. Phys. A (to be published), hep-ph/0303186.

[13] W. Beenakker, W.L. van Neerven, R. Meng, G.A. Schuler, and J. Smith, Nucl. Phys. **B351**, 507 (1991).

[14] N. Kidonakis, hep-ph/0208056.

[15] W. Beenakker, H. Kuijf, W.L. van Neerven, and J. Smith, Phys. Rev. D **40**, 54 (1989).

[16] A.D. Martin, R.G. Roberts, W.J. Stirling, and R.S. Thorne, Eur. Phys. J. C **28**, 455 (2003).

[17] CTEQ Collaboration, H.L. Lai *et al.*, Eur. Phys. J. C **12**, 375 (2000).

[18] J. Pumplin, D.R. Stump, J. Huston, H.L. Lai, P. Nadolsky, and W.K. Tung, J. High Energy Phys. **07**, 012 (2002).

[19] N. Kidonakis and J. Smith, Phys. Rev. D **51**, 6092 (1995).